

1.1. FSD or FTD

1.1.1. WPBB: Work Package Breeding Blanket

1.1.1.1. *Analysis on surface effects in view of tritium permeation assessment for niobium and vanadium [BB-S.05.01-T003-D008]*

The hydrogen and deuterium permeation in pure niobium and niobium Pd25%Ag coated are measured using a permeation gas phase technique. The coating with different thicknesses, are deposited on Nb by a Dual Ion Beam Sputtering Technique.

Measurements are performed in the temperature range of 573 – 723 K with hydrogen or deuterium driving pressures in the range $1.0 \cdot 10^2 - 1.2 \cdot 10^4$ Pa (1 to 120 mbar). This work highlights how PdAg-coated Nb membranes can be fruitfully rated in the design of tritium recovery plants where niobium pipes for lead lithium are under consideration. Ultra-thin PdAg coatings mitigate the effects of the oxide in reducing of hydrogen permeation through the niobium walls.

Experimental

Table 1: Sample name, membrane structure and deposition parameters of PdAg coating. E_b is the beam energy, J_b the beam current density and d the PdAg film thickness. Nb_2O_{5-x} is for niobia, a mixture of NbO, NbO2 and Nb2O5 this last is the most stable oxide with the smallest formation energy.

Sample	Membrane structure	E_b (eV)	J_b ($\mu A/cm^2$)	d (nm)
A	PdAg/Nb/ Nb_2O_{5-x}	500	45	$\simeq 110$
B	PdAg/Nb/PdAg	500	45	$\simeq 55$
C	PdAg/Nb/PdAg	500	45	$\simeq 110$
D	PdAg/ Nb_2O_{5-x} /Nb/ Nb_2O_{5-x} /PdAg	500	45	$\simeq 110$
E	Nb_2O_{5-x} /Nb/ Nb_2O_{5-x}	–	–	0

The membranes are disks with a diameter of 25 mm obtained from a thin niobium sheet thick 0.5 mm. Some membranes have been realised by depositing a PdAg film with 25% in Ag mole, on one face of the niobium disc. In this case, the PdAg film dissociates molecular hydrogen into atomic hydrogen, which diffuses in the film by reaching the niobium. In this way, the diffusion process is similar to that in PAV where only niobium is used for separating PbLi from vacuum.

To compare permeation between membranes in which niobium was not oxidized to those obtained using naturally oxidized niobium disk, samples have been realized where the PdAg film is deposited on the still-oxidised face and others in which the oxide has been removed before deposition.

Samples have also been realised in which both non oxidized faces of the niobium disc have been coated with a PdAg film. These type of membranes relates to the case where the tritium recovery section was designed by using coated niobium with a PdAg film on the vacuum side of the PAV.

1. EUROFUSION

Results and discussion

Permeation measurements were performed on sample A with only one face coated. This sample is representative of a framework where the PAV walls are made of niobium, meaning not pure niobium but of a material with at least one oxidised surface. In fact, our source is molecular hydrogen that is dissociated from PdAg and diffusing in niobium. The uncoated wall of sample A, being exposed to air, oxidised naturally. Measurements were taken in the range of 573 K to 723 K at a pressure of $15 \cdot 10^2$ Pa because these values roughly correspond to those of PAV design.

The fluxes measured in sample A are shown in Fig. 1. The same measurements were made on sample C, which corresponds to a design in which the PAV wall faced to vacuum is coated with PdAg. The fluxes measured in sample C are about 40 times larger than those in sample A at $T = 723$ K. The fluxes ratio for the two membranes is about 600 at $T = 573$ K. In the same figure, the deuterium flux, permeated through bare niobium sheet 0.5 mm thick, (sample E) is reported for comparison.

For sample E, the use of deuterium instead of the hydrogen is due to the low value of the permeated flux that is very close to the limit of detectability of the experimental set-up. In this way, the deuterium detected at the permeate side can come only from the feed side without possible contamination. On the other hand, quadrupole mass analysis confirms that the permeated gas is only composed by deuterium.

In the sample E, the measured flux is very low and it is more than four orders below the flux measured in sample C. These measurements demonstrate the advantage of considering Nb/PdAg membranes in the design of the tritium recovery system with the coated surface facing the vacuum and the Nb surface wetted by PbLi.

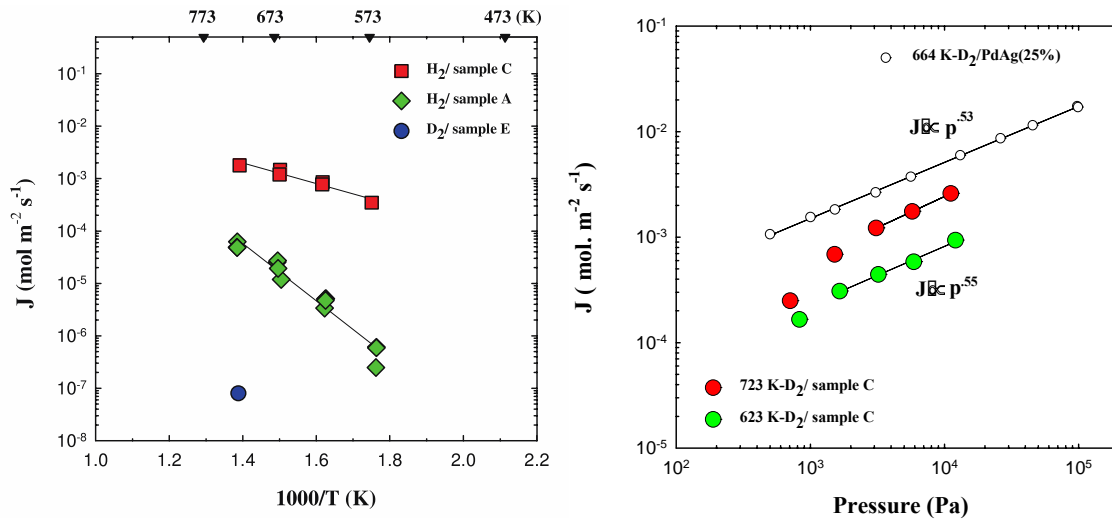


Figure 1: (left side): Hydrogen permeated flux of membranes A and C in Tab.(1). Green diamond and red square are fluxes measured respectively for membrane A and C. Blue circle symbol represents deuterium permeated flux of as received niobium disk naturally oxidized; (right side): Dependence of deuterium flux with the pressure at the steady state for membrane C (tab.1) at 623 K, green circles, and 723 K red circles. The black open circle symbol is related to the results reported in ref. [1] for a Pd25%Ag membrane.

The increase of permeated hydrogen flux has been noticed for two kinds of membranes, B and C of Table 1, after few thermal cycles at a pressure of $\overset{\llbracket \llbracket}{\text{SEP}} \approx 15 \cdot 10^2$ Pa. In particular, the membrane B (PdAg film thinner) reach the stationary state after three cycles whereas the membrane C (PdAg film thicker) after two cycles.

The measurements show that the thickness of the PdAg film is not so critical for membrane performance. Reducing the coating thickness by 100% did not change the flux value. These results encourage further investigation to determine the minimum thickness of the PdAg film for which J begin to have lower values.

Figure 2 reports the steady state deuterium flux through the membrane C versus the pressure at two different temperatures, 623 K, green circles and 723 K, red circles. For comparison, in the same figure is reported the behaviour of the flux versus the pressure of a Pd25%Ag membrane published by ref. [1]. The dependence of the flux J on pressure p, in the case of negligible surface effect, follows $J = (P/t)p^{1/2}$ law, where P is the permeability and t is the membrane thickness. The same behaviour can be qualitatively assessed for the membrane C, where the dependence of the flux on p shows two different behaviours. At the low pressures (≤ 1 kPa), the flux-pressure dependence approaches $\approx p^1$, while at the high pressures, the flux dependence approaches $\approx p^{0.5}$.

In figure 3, the deuterium permeability P of membrane C are compared with the permeability reported in literature for Pd25%Ag membrane [1], bare niobium sheet [2] and niobium membrane E (Table 1). As can be seen, the deuterium permeability at $T \approx 723$ K of a bare niobium (membrane E of Tab. 1) increases more than four order of magnitude by depositing on both sides a Pd25%Ag layer thick ≈ 110 nm. $\overset{\llbracket \llbracket}{\text{SEP}}$

The values measured at $T = 723$ K on the niobium membrane (sample E) are about two orders of magnitude lower than those measured by Malo et al [2] although it is not clear whether their results are obtained using deuterium in atomic form. The experimental results reported in Fig. 3 confirms what the authors of Ref. [2] themselves state, namely that the oxidation conditions of the niobium surface can significantly alter the value of the expected flux. This is also true for membrane A where only one side is oxidised.

At fixed temperatures, permeability (P) of the membranes monotonically increases if we consider the membranes according to the following sequence: 1) uncoated Nb membrane (sample E), 2) one side coated but the other oxidised (sample A), 3) both sides coated but the niobium is oxidised (sample D), 4) both sides are coated but PdAg has been deposited on pure Nb (Sample B and C).

In the membrane D, the PdAg coating promotes permeability despite the niobium being oxidised. This is most likely due to the implantation of PdAg in the oxide layer. For this reason the P measured in membrane A is still almost $\overset{\llbracket \llbracket}{\text{SEP}}$ 1 order of magnitude lower than that measured in sample D.

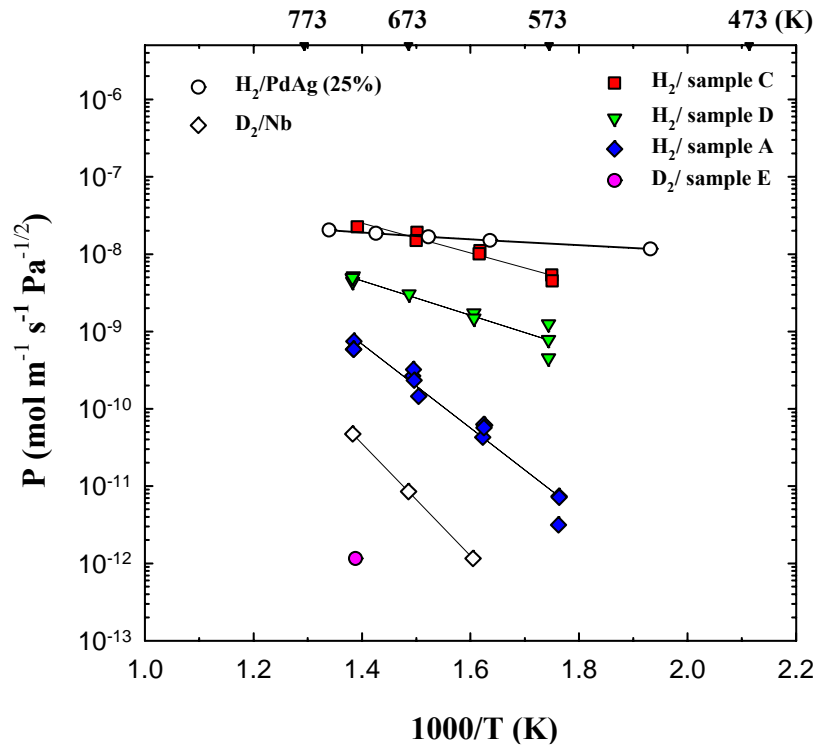


Figure 3: Hydrogen permeability measured in membrane A (blue diamond), C (red square), D (green down triangles). Deuterium permeability measured in membrane E (violet circle). For comparison, hydrogen permeability in Pd/25%Ag membrane reported in Ref. [1] (black open circle) and in bare Nb sheet reported in Ref. [2] (black open diamonds).

With a view to realising a tritium recovery system, the use of membranes with characteristics that do not depend on surface properties is highly desirable. Coating niobium can resolve inhomogeneities related to its oxidation and surface morphology also in view of the fact that the tritium recovery facility can be quite large. The use of ultrathin PdAg films shows an increase in the permeability value to values comparable with those of a PdAg sheet membrane. The repeatability of the results in PdAg-coated membranes goes in the direction of being able to have more reliable values for the WCLL design.

References

- [1] E. Serra, M. Kemali, A. Perujo, D. Ross, Hydrogen and deuterium diffusion in the Pd-25%Ag alloy, *Metall. and Mat. Transactions A – Physical Metallurgy and Material Science* 29 (1998) 1023–1028.
- [2] M. Malo, D. Garcinun~, D. Rapisarda, Experimental refutation of the deuterium permeability in vanadium, niobium and tantalum, *Fusion Engineering and Design* 146 (2019) 224–227.

1.1.2. WP DIV –DEMO

1.1.1.2. Preliminary joining technologies for pipes of dissimilar materials_2022 [DIV-DEMO.T.1-T009-D001]

The preliminary investigation on dissimilar welding of CuCrZr to Martensitic creep resistant steel was done during 2022. The direct welding of copper to steel results to be a difficulty with high susceptibility to the formation of brittle microstructures and cracks that are not allowed, specially, for structural application. The employment of transition alloy, such as Inconel 625, promises to overcome the problem about the embrittlement of the joint. The Laser welding, especially if further assisted by Hot Isostatic Pressing (HIP), , could be the candidate fabrication process to make the transition EUROFER manifold between the CuCrZr pipe of the target and the main manifold of the cooling system of the Cassette Body (CB). The HIP treatment is useful to reduce porosity and residual stress and moreover perform post welding process to recovery ductility and strength in both steel and copper side

The DEMO fusion reactor use of magnetic fields allows to manage the plasma in such a way that the contact between the latter and the toroidal chamber should be limited to a certain region only, namely the divertor region. Figure 1 shows a CAD representation of DEMO and its divertor [1].

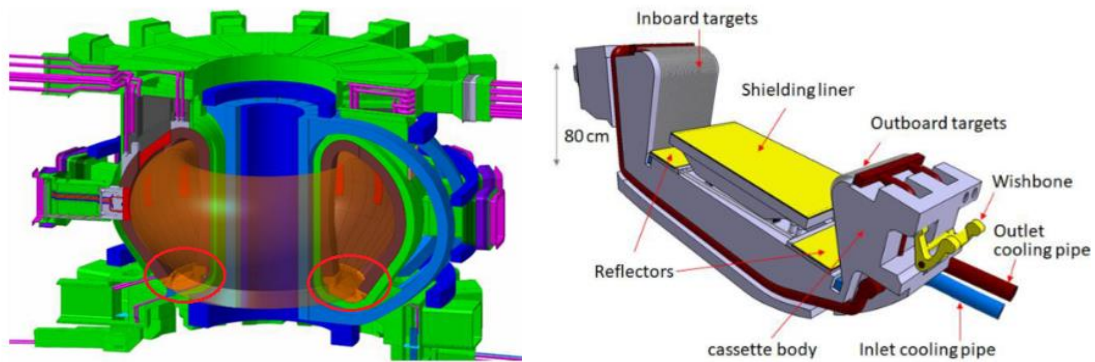


Figure 1: DEMO CAD representation and particular of the divertor cooling system [1].

The components to construct the divertor are special small tungsten blocks for the outboard and inboard targets (Figure 2). Inside these small blocks, a cooling pipe made of CuCrZr is joined by diffusion bonding.

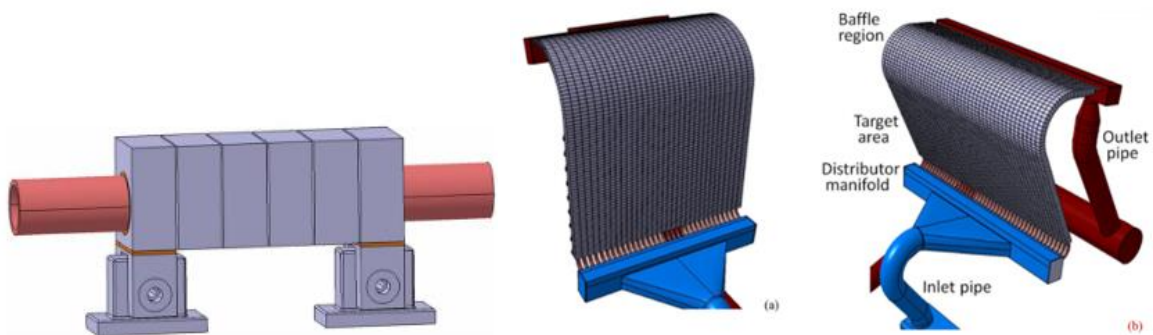


Figure 2: SX: target element segment schematization; DX Targets compelte [1].

1. EUROFUSION

One single target will be composed of many of these cooling channels in parallel which will then be joined to the main cooling pipe by welding the single cooling channel to a manifold. The current candidate material to make the manifolds and pipes is EUROFER 97, therefore to produce the CB it is necessary to develop a transition joint between the CuCrZr cooling pipes of the target and the manifolds.

The approach is to develop a transition joint on the CuCrZr, 15 mm outer diameter (OD) target pipe and a portion of pipe made of EUROFER 97. For preliminary development of the welding process a High Density Energy process was selected (LASER welding) and due to the reduced availability of the EUROFER 97 a similar surrogate creep resistant steel (P91) was used for the research.

State of the art of dissimilar welding of copper to steel

Dissimilar joints have been the object of study in many research activities due to their possible extensive use in many fields of technology. A lot of combinations were studied among various metals such as copper, aluminum, stainless steel, titanium etc. A lot of attempts of laser welding stainless steel to pure copper have been made. Currently, concerning especially joints between steels and copper alloys, the most studied is the butt joint between these two materials. Kuryntsev et al. [2] used a defocused beam and the offset was put on the steel, in order to avoid excessive melting of copper. By using this method, no cracks or pores were found in the butt joint. This research confirmed that putting beam offset on steel in dissimilar steel-copper welds can be a valid choice to avoid excessive melting of the copper, intergranular penetration and the consequent penetration cracks. Sahul et al. [3] reports that the best result was obtained with the focused laser offsetting the welding line on Cu side, both in terms of shape and strength ($R_m > 250$ MPa was obtained in tensile tests).

The welding of creep resistant steel P91/ Eurofer97 to Copper it is not recognized in literature because it is more hard to obtain due to martensitic microstructure of these steels that are made without Nickel. Therefore many solutions were designed and investigated. The Figure 3 summarizes the evaluated solution.

Esperimatal Test

The welding test was performed using a laser gantry workstation of the Laboratory Material and Chemical & Physical Technologies of ENEA (SSPT-PROMAS-MATPRO).

The main features of the welding workstation are:

- Collimator focalization: $f_c=100$ mm;
- Work Fiber diameter: $dk=100$ μ m;
- Focusing lens: $f=250$ mm;
- Nominal diameter of focal spot: $d_0=250$ μ m

A rotating axis and a wobbling welding head were used. To allow the welding and protect the welding seams during the process, a specific equipment was used, consisting of an aluminum pipe with a closed extremity which allows it to be filled with argon; on the other side a plastic ring with a precise hole (diameter 15,5 mm) is applied to consent at the same time the rotation of the pipes and a good filling of argon. The Figure 4 shows the equipment and the welding SET-UP.

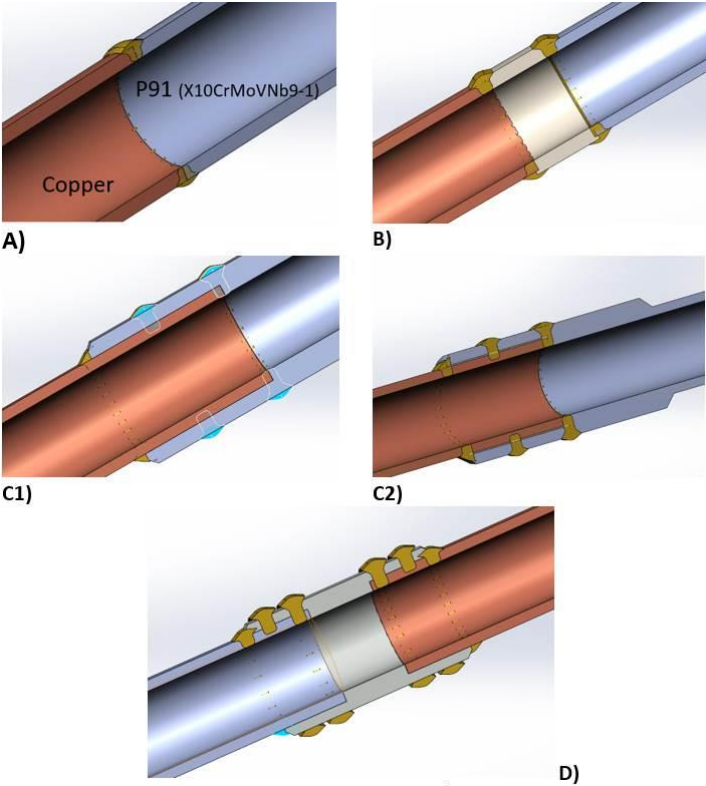


Figure 3: Scheme of the joint configurations

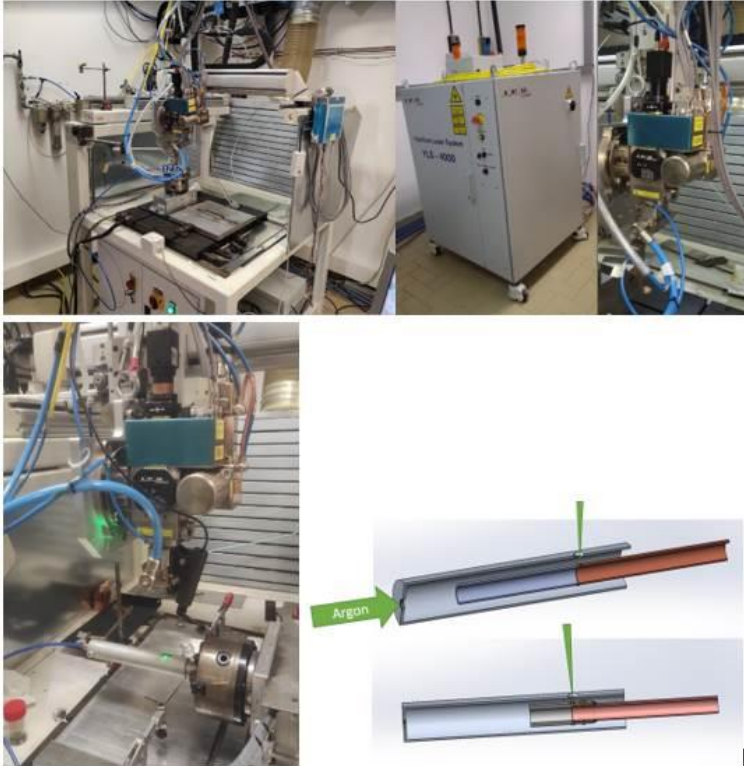


Figure 4: ENEA laser welding workstation 500x500x300 mm plus rotating axes; laser source IPG YLS-4000 CW and wobbling welding head, scheme of the shielding system.

All the configuration of the Joint were tested supporting the laser welding process with components made by MFFF 3D printing for the Inconel 625 transition parts and Hot Isostatic

1. EUROFUSION

Press (HIP) to improve the features of the joint. A lot of test, to identify good welding parameters, in terms of power, focusing and wobbling were performed and analyzed using Design of experiment. The summary of the main result in terms of visual examination and macro cross section are reported in the following pictures.

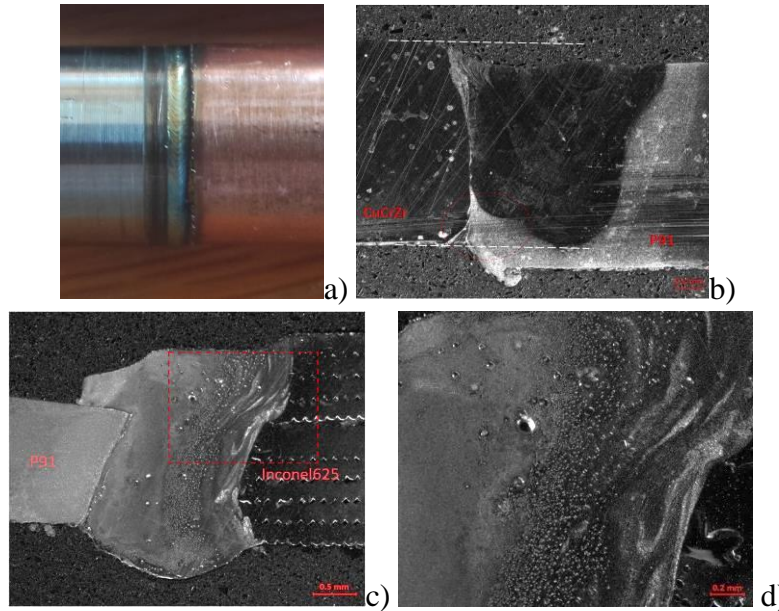


Figure 5: BUTT JOINT (a & b without interlayer) (c & d) with Inconel 625 Interlayer

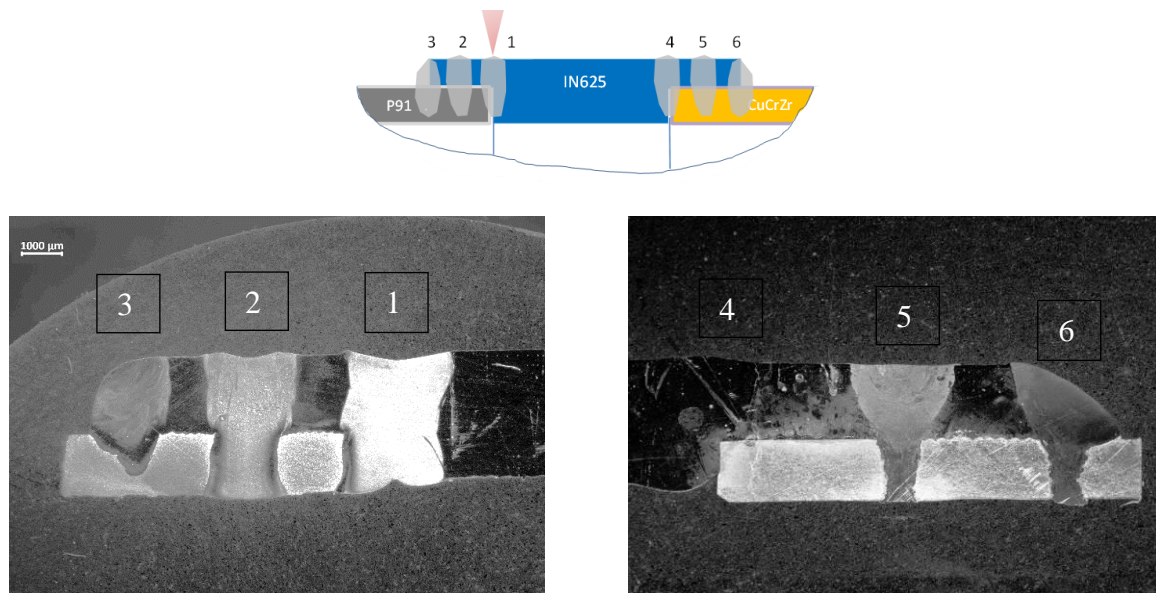


Figure 6: Scheme and example of LAP Joint with Inconel 625 transition ring

Characterization

On the promising welded coupons, Digital Xray, micro hardness and SEM analyses were done to evaluate the quality of the joint and understand some mechanism of formation of porosity and cracks. An example of the examination performed is summarized in Figure 7.

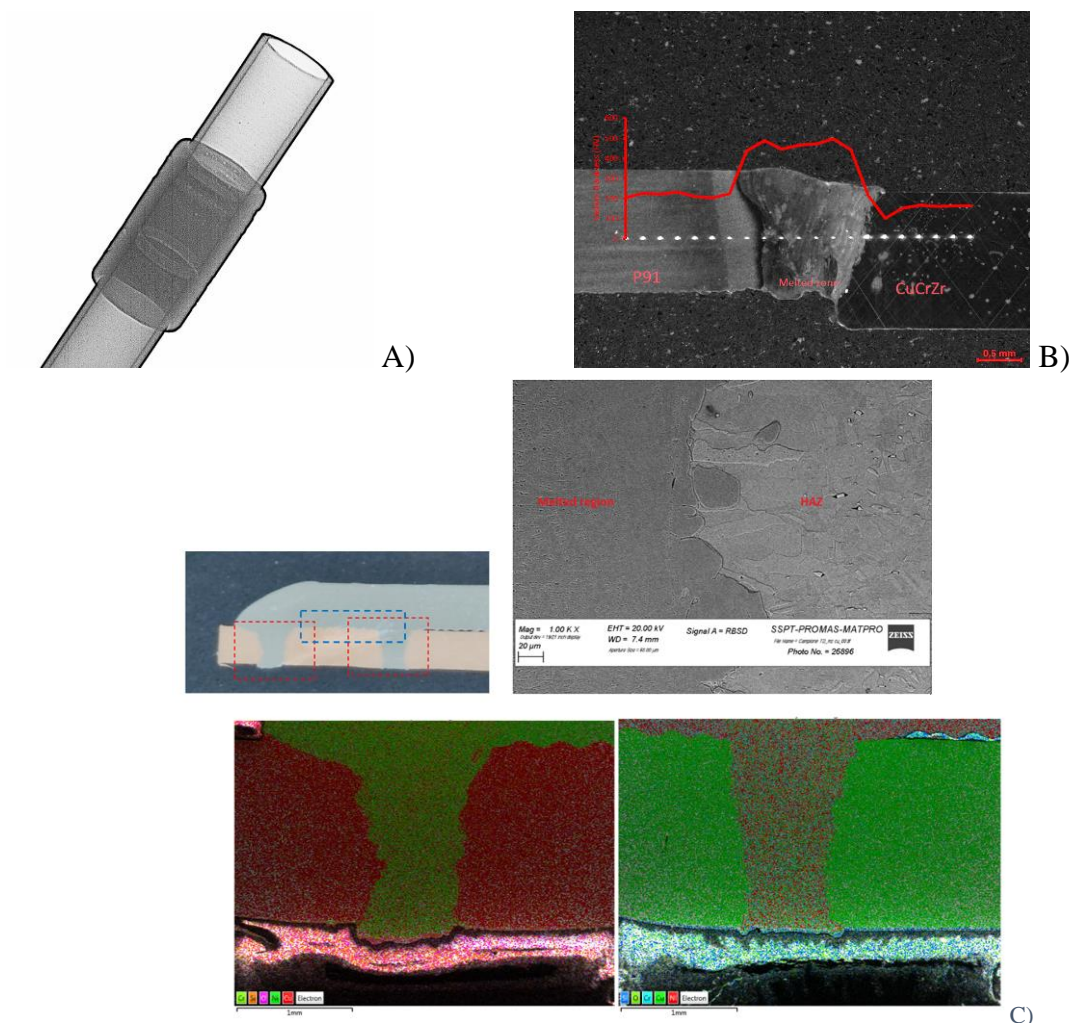


Figure 7: example of characterization of welded pipes coupons: A) Digital Xray examination that allow to evaluate the presence of porosities and macro cracks; B) micro hardness tests to evaluate the formation of hard and brittle microstructure or softening in HAZ; C) SEM and EDS analyses

Conclusion

During 2022, several solutions to the problem of dissimilar joints in DEMO divertor have been investigated. The research started with the simplest possible configuration (butt joint) and then took into account other solutions in order to cope with this crucial issue. In the beginning, butt joints seemed to be a possible solution since in the last attempt, playing with values of laser power and offset, the joint seemed to be good. Nevertheless, SEM investigation of the butt joint specimen revealed that lack of adhesion was still present, even though it was of minor size with respect to the first butt joint attempts. Lap joints could have been a valuable solution; nevertheless, cracks in the joint Solution C1 and C2 attempts were found. The insertion of an interlayer of Inconel625 resulted in an insufficient improvement since it was unable to prevent iron and copper from mixing up during the lap joint process. The solution B and D, seemed to give satisfying results. No cracks were detected right after

1. EUROFUSION

the joint and the different elements (copper, iron and nickel) mixed homogeneously together without creating any compatibility problem.

This leads to conclude that the dissimilar joint performed using a transition ring or manifold for the lap joint made of Inconel625 between the P91 and CuCrZr pipe are up to now the most promising solutions.

To improve the result and quality of weld it is necessary to abandon the solution of printed transition material Inconel625 by MFFF that even if rapid and flexible to realize the components for this preliminary evaluation, due to the not fully density and residual binder material introduces an ulterior variable in the developing of process.

Moreover, the specific tolerance and design of ring and manifold are necessary, so the next step of the work needs to have realized the part from an external workshop.

The last solution D demonstrates that the welding seams are of good quality and correctly sealing the portion of the pipe in the middle because the HIP process allows the bonding of the Cu alloy to Inconel625 manifold. If linked pores or cracks were present trough the thickness around the welds, the high pressure Argon filling in the interface of the pipes would hinder the bonding process. Moreover, the HIP allows to perform a reduction of porosity actually induced on laser welding process.

The microhardness tests confirm the formation of metastable and brittle microstructures when Fe and Cu were mixed, moreover the copper alloy evidences a softening of about the 30% in hardness. This means a reduction of tensile strength. On the other side, the P91 increases, in particular in HAZ, the hardness, so, it could became brittle: the development of an adequate PWHT needs to be investigated with the objective to reduce both the softening in HAZ of CuCrZr and the hardening of P91/Eurofer.

In the event that it is not possible to adequately recover the softening in CuCrZr HAZ, it will be necessary to evaluate a re-engineering of the joint.

So, in general, laser welding with Inconel as transition material, assisted by HIP, promise to make adequate joint of EUROFER to CuCrZr.

References

- [1] G. M. e. a. J.H. You, «Divertor of the European DEMO: Engineering and technologies for power exhaust.».
- [2] A. M. A. K. G. S.V. Kuryntsev, «Fiber laser welding of austenitic steel and commercially pure copper butt joint,» Optics and Lasers in Engineering, vol. 90, pp. 101-109, 2017.
- [3] T. E. S. M. P. M. L. B. H. E. .. Sahul M, «Effect of Disk Laser Beam Offset on the Microstructure and Mechanical Properties of Copper—AISI 304 Stainless Steel Dissimilar Metals Joints,» Metals. , 2020; 10(10):1294.

1.1.3. WP DIV-IDTT

1.1.3.1. *Conceptual design of in-bore cut_&_Weld_tools and related interface and requirements management [DIV-IDTT.S.04-T012-D001]*

The work describes the activity done for identification of the basis configuration of laser cutting and welding tools. Starting from some test performed by a standard laser cutting machine, a roughness assessment was performed to identify the best laser source for the cutting process. However, the result is not fully reproducible by an in bore cut system due to the limited dimension. Market research put in evidence that the standard Cutting and Welding Head cannot be applied and needs a fully redesign starting from elementary optic. Even in this case the limited dimension inside the pipe, further reduced due to the necessity of overcome pipe curves, do not allow to obtain the optimal focusing parameter (Like Z_r and D_0).

The preliminary identification of laser power, considering a thickness of 3 mm of the pipe wall, was done; at the same time to ensure reproducibility and optimal geometry on the cutting and welding area a special portion of tolerated pipe was considered. In the same zone an additional external shielding pipe is necessary to avoid damage of internal component due to excess of laser energy.

A shielding system has been hypothesized for the Cutting and Welding Area.

Replacement of the In-Vessel components of the DTT facility requires the connection/disconnection of the cooling system pipes. Given the limited space inside the VV and also outside, it is not always possible to open the duct flange (ex NBI) and act from outside of the pipes for cutting and welding.

For this reason it is necessary to develop an in-bore welding tool capable of cutting and then re-welding pipes at a later stage. Moreover, given the interferences with the various components in cutting and welding areas, it is not always possible to use the robotic arm to align the pipes (in red the cutting zone).

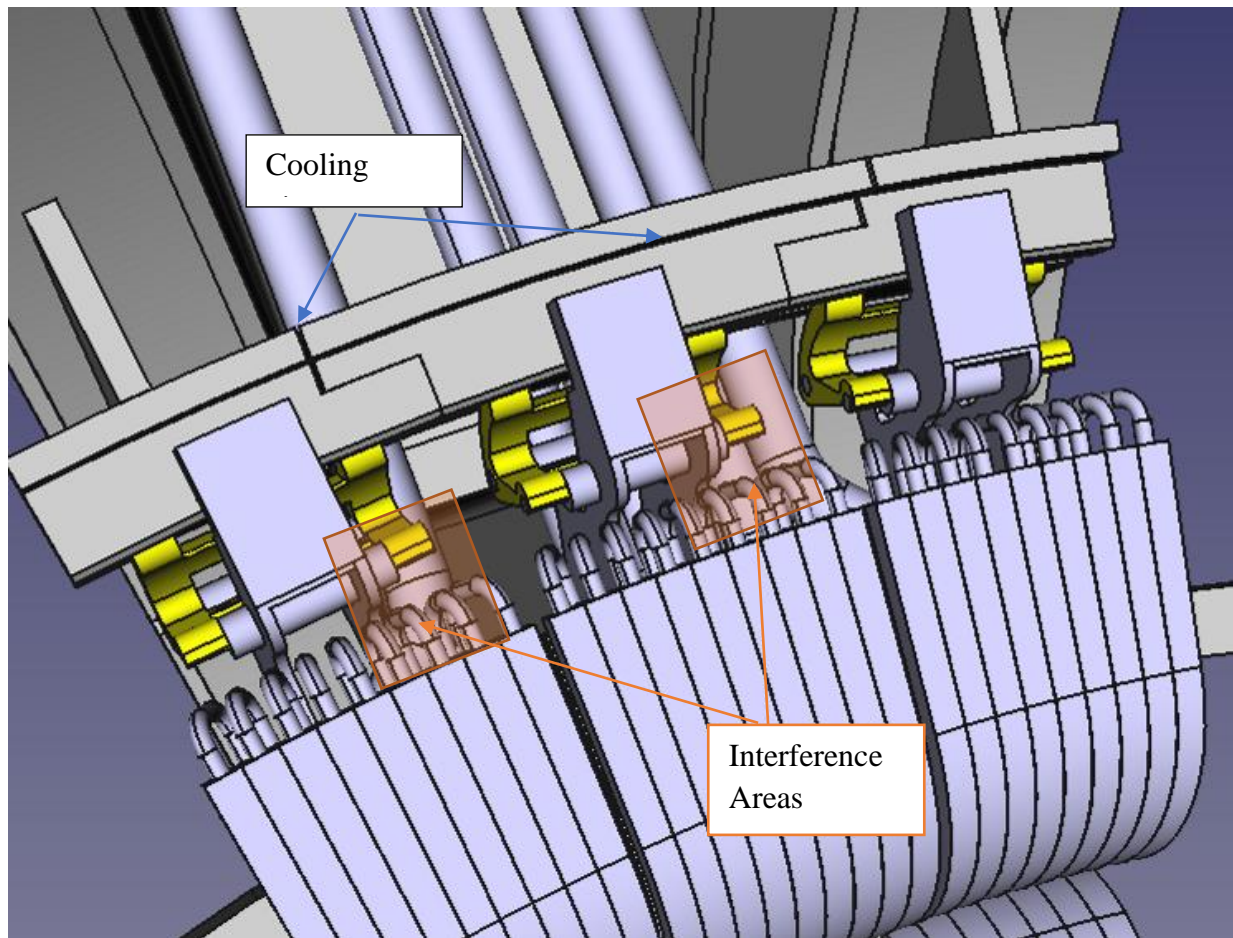


Figure 8: Rendering of a portion of “DTT “cassette” with indication of cooling pile and interference one

To allow the toroidal translation of the cassette with the CTM, the tube must be cut inside the VV, so that the stump of tube left on the cassette does not create collisions during RH operations. For this reason, the developed tool has an in-bore alignment system on board.

The objective of the work can be synthesized as follow:

- Definition of functional and design requirements for cutting and weld in bore tools;
- Interfaces Definition;
- Feasibility analysis;
- Preliminary Mechanical concept of the C&W (cut/weld/inspection/alignment/ etc);
- Preliminary design of the Control logic of the C&W, sensing, monitoring, commanding and Control;
- Update of the Design requirements;
- Update of the preliminary design of the Control logic of the C&W;
- Conceptual design of the C&W device. Description of Results

The main pipe diameter of DTT cassette cooling system is (OD) 60 mm and the thickness is 3 mm.

Literature analysis

A preliminary analysis of similar tools in literature has been carried out. The papers of S. Kirk & others of United Kingdom Atomic Energy Authority, Cranfield University and TWI, study “In-bore Robotic Laser Cutting and Welding Tools for Nuclear Fusion Reactors” and report interesting result about in bore cutting and welding in on pipe of 90 mm of diameter and 5 mm of thickness. The work of Kirk & others applies to the concept of develop a novel miniaturized laser processing head design for in-bore laser cutting and welding [1] [2] [3].

Takao Hayashi & other study the cutting in bore tools by milling [4]. The following pictures summarize the cutting tool developed from JAEA. The dimension of the pipe is similar to DTT (OD 59,8 mm, t= 2,8 mm) however the positioning of cutting and welding zone is extremally easier in the JT-60SA design than DTT.

The design of cooling duct in JT60-SA allows to use a straight tool, both for cutting and welding. This thanks to the access through a “plug”. The same research group develops an in-bore welding tool [5, 6, 7]. Similarly the level of flexibility and difficulty of this tool compared to those needed for DTT is an order of magnitude easier.

The welding tools of JT60 -SA is straight with a diameter of 36 mm to weld a similar pipe of DTT (OD 59,8 mm; t=2,8 mm).

The laser source applied is a CW 4 kW fibre laser and the focused beam on the internal pipe was 1,2 mm of diameter. Note that this is not standard focused beam diameter dimension for laser welding, however, in similar way of the work of S. Kirk & others [4], this is probably the best compromise between the miniaturization of the internal laser head and the optimal laser welding parameter for this particular application.

Starting from the literature information, we found some interesting information about the miniaturized laser cutting/welding heads. The available data about laser parameter for cutting and welding that can summarized as follow:

- Cutting: Laser spot 0,7 mm; Power 1,2 kW; t=5 mm; ID 90 mm; speed process 8 mm/s
- Welding: laser spot 0,7-1,2 mm; power 2,2-3,4 kW; t=3mm; ID 90 mm / OD 59,8; speed 8 - 14 mm/s

Some industrial laser cutting tests were performed thanks to the support of the Workshop of IPG Photonics Italy.

Esperimatal Test

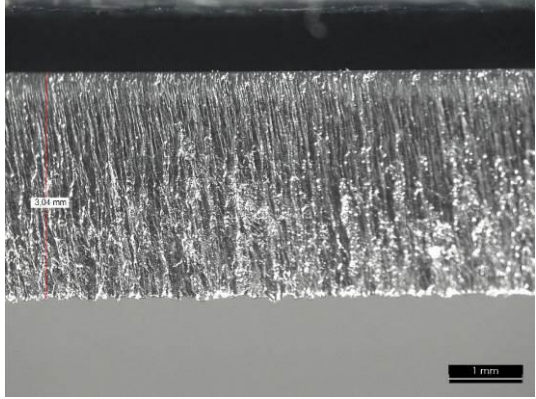
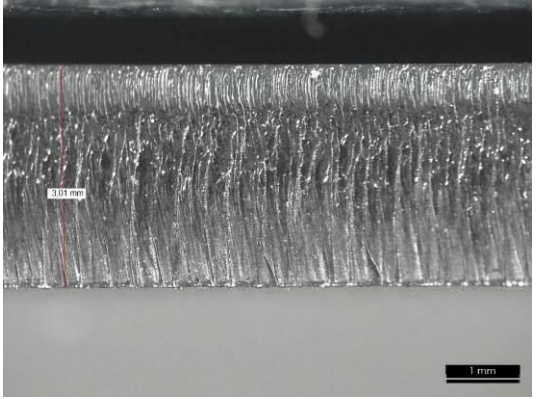
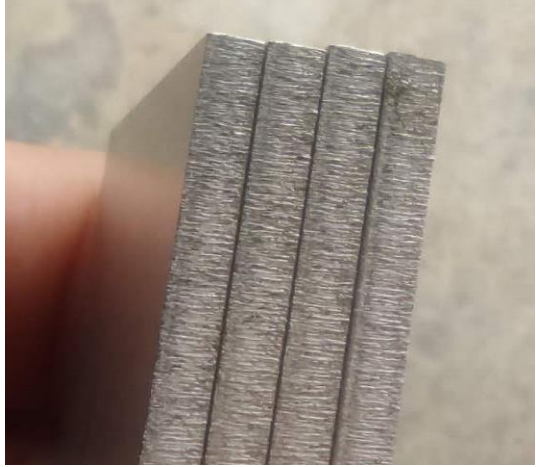
Some cutting tests on 3 mm thick stainless steel plate were performed. The main parameters have been summarized in the following table.

The starting area of the machining is highlighted in the red circle where a small difference in the kerf is evident which must be taken into consideration in a circumferential laser cutting machining.

The cut surface was analyzed using a 3-D optical profilameter (New View 5000, Zygo Corporation, USA).

1. EUROFUSION

Table 2: Summary of main cutting parameters whit pictures

Laser source	YLM- QCW 450/4500	YLS -2000- SM
Power	450/4500	2000W
Speed	17 mm/s	100 mm/s
		
		

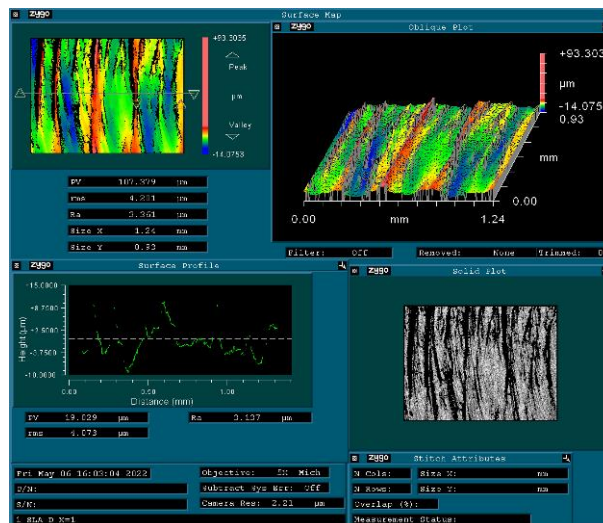


Figure 9: example of Roughness analysis of the cut edge

Welding tests were performed using a gantry laser station of the ENEA Chemical-Physical Materials and Technologies Laboratory (SSPT-PROMAS-MATPRO). The parameters have been summarized in the following table.

Table 3: Summary of Laser welding parameter

ID 61 C	Power [W] – Pulse time [ms]	Wobbling (shape/width[mm]/frequency[Hz])
I	2000 CW	NO
II	1500 CW	NO
III	0/3000 - 2/4 ($P_{av}=2000$ W)	O/0,25/24
IV	0/2250 - 2/4 ($P_{av}=1500$ W)	O/0,25/24

The appearance of CW on the left is very good, perfectly protected on the cap and on the rear of the welded seams.

The “III” and “IV” seams were performed at the same average Power respectively of “I” and “II” but with modulate power with a frequency of 166,67 Hz and with circular wobbling. This modulated wave should be useful to reduce the porosity typical of keyhole laser welding on SS 316.

The digital X ray examination was performed on the whole welded plate. The examination reports some porosity on seam “I”, diffuse porosity on seam “II” with an increasing of the thickness in the centre of welded seams due to the swaging effect.

The modulated welding parameter induces a reduction of the porosity in the "III" bead however undercuts and spatters are highlighted in the macro cross-sections (Figure 10).

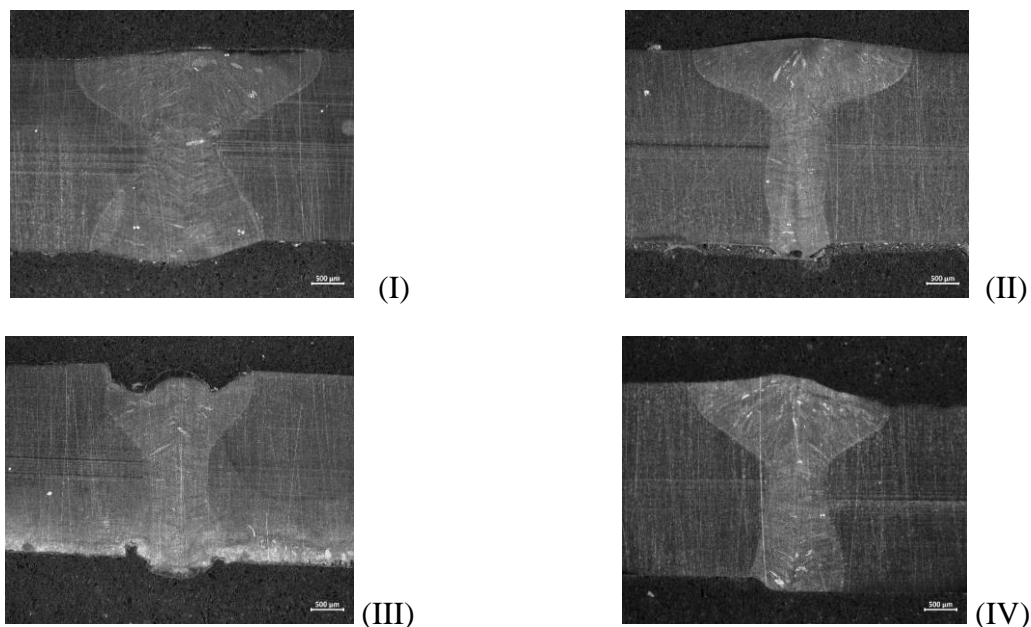


Figure 10: Macro cross section of the weld seams

1. EUROFUSION

Preliminary mechanical concept of the C&W

Based on the literature review, tests with standard industrial equipment and market research were performed. Industrial solutions for in-bore cutting and welding tool for DTT cannot be found and applied, but the constraint for designing a good tool has been identified.

We need to take in consideration the follow requirement:

- Develop solutions to cut and weld close to curves;
- Align the pipes from the inside with a max axial misalignment <0.2mm and a max gap < 0.3mm.
- Maximum external diameter of the pipes to be welded 60 mm.
- Full penetration welding of 3 mm thick pipes;
- Welds that can be inspected by NDT;
- Protection of the outside pipe components in the VV from possible excess of laser beams power/fumes/spatter both after cutting and welding processes.
- “Zero gravity” condition for cutting process, to avoid final cracks\ excess of deformation and defect at the end of the process;
- Mechanical finishing of the laser cutting edges;
- Visual or proximity sensor for individuate the cutting/welding line;
- Low resistance force to move the pipe to be welded in the duct (translation of the pipe in the duct normal to the surface to be welded) – the cut/welding tool is designed to apply 15 kg of force to join the pipes together and 15 g to reduce the misalignment.
- After being cut, the pipes must not put the internal part of the VV in communication with the hall.
- Welding is possible, even with a modified pipe length following a cutting operation.

A preliminary scheme to make cutting and welding possible and repeatable is shown in the following figure.

Analyzing the focusing system it is possible evaluate the Rayleigh distance (Z_R , where the beam cross-sectional area doubles).

Table 4: Summary of formula for the parameter for design the focusing head

L	d0	ϑ	zR
$f \frac{x^2}{x-1}$	$\frac{\Phi}{x-1}$	$\alpha(x-1)$	$\frac{\Phi}{\alpha} \frac{1}{(x-1)^2}$

f: focal lens distance, **Φ:** fiber diameter, **α:** divergence out of the fiber, **x = p/f**

The Z_R is an important parameter because it quantifies the stability of the diameter of the focused beam and it is good that it is of the same order of magnitude as the thickness.

Due to the small diameter of the tube, the configuration with $x=2$ (which gives rise to the minimum total axial dimension) results in a Z_R of less than 1 mm. To increase Z_R up to 2 mm the x need to be set at 1,62. In this case, some possible plano-convex lenses were evaluated to create the in-bore focusing system.

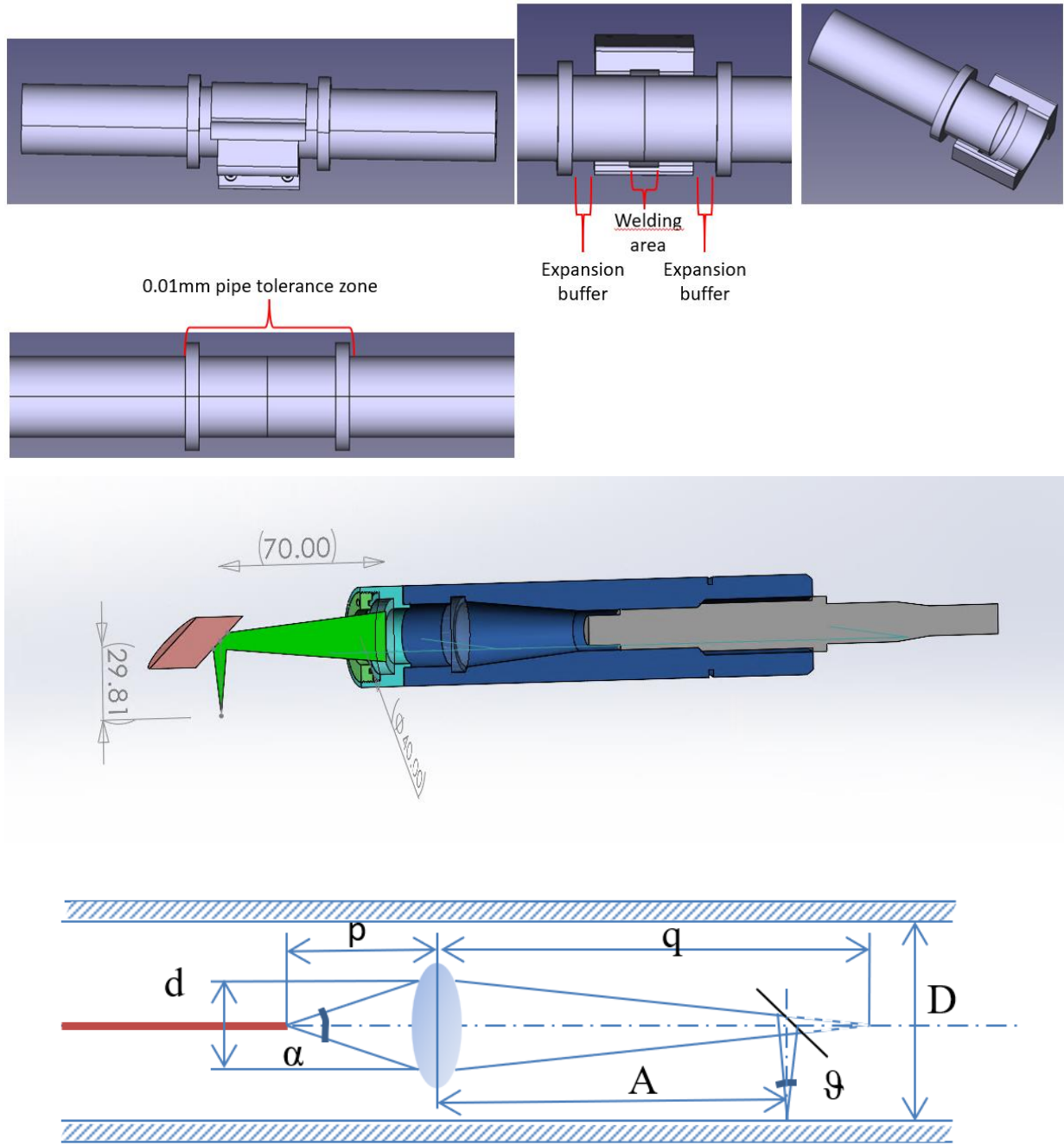


Figure 11: Schematization of in bore C & W focusign constrain and design.

Table 5: Selection of plano-convex lenses: Thorlabs catalog, 400-1100 nm coated N-BK7

type	d lens (d usable)	f	L	D
LA1540-AB	12,7 (8,9)	15	63,5	3,2
LA1074-AB	12,7 (8,9)	19,9	84,2	4,2
LA1560-AB	12,7 (8,9)	25	105,8	5,3
LA1951-AB	25,4 (17,8)	25,4	107,5	5,3

(The last two lens, grey boxes, overcome the threshold limit)

1. EUROFUSION

Conclusions

A state of the art about the in-bore cutting and welding system for maintenance of cassette of Divertor of Fusion reactor and experiment was done.

Despite the literature papers, the design of cooling system of the DTT impose to design a snake in bore cutting and welding system. The dimension in terms of diameter of pipes is similar to the Japanese JT 60 -SA, however the design of the Divertor and cassette cooling system of the JT 60 allow to operate in an easy way by a straight tool.

The tools developed from Kingdom Atomic Energy Authority is more flexible but it is designed for larger piper (ID 90 mm) and to overcome curves in the cooling system with larger bending radius (1200 mm) than DTT (450 mm).

The study of literature allows to confirm some initial consideration:

- Outside Shielding system;
- Cross jet;
- Positioning sensor and calibrate zone for cutting and welding.

However not all the informations are available in literature. For example, the quality of the cut in the UK paper is very bad and the test about welding are probably performed with milled edge. More complete information is retrieved in the study of in bore welding the paper of JAEA.

The Experimental study performed at ENEA allows to evaluate the features needed for the laser source.

An IPG YLS 2000 laser is appropriate both for cut and welding but a solution with CQW for cutting with a working fibre below the 100 microns should give small kerft.

At 0,6 m/min the 2 kW welding test, performed with defocusing simulating a theoretically miniaturized laser head, promise an acceptable quality of welding.

A conceptual design of the holding, aligning, and shielding system in the zone of Cutting and welding was designed.

Potentially exist the single lens and or mirror but to overcome the curves in the cooling system of the DTT, it is probably needed do develop a spitted cutting and welding head.

We are starting to contact developer of industrial laser system (like IPG, El.EN and Precitec) to individuate a candidate to realize the prototype of the optical configuration.

References

- [1] K. K. W. S. T. T. C. A. I. F. S. Kirk, «Remote in-bore laser cutting and welding tools for use in future nuclear fusion reactors,» in WM2018 Conference, March 18 – 27, 2018, , Phoenix, Arizona, USA, 2018.
- [2] K. K. L. N. a. T. T. S. Kirk, «In-bore Robotic Laser Cutting and Welding Tools for Nuclear Fusion Reactors,» Lasers in Engineering, vol. 46, 2020.
- [3] «Novel miniaturized laser processing head design for in-bore laser cutting and welding,» UKAEA, 2021. [Online]. Available: <https://scientific-publications.ukaea.uk/papers/novel-miniaturized-laser-processing-head-design-for-in-bore-laser-cutting-and-welding/>. [Consultato il giorno 10 11 2022].

- [4] S. S. K. S. A. S. Takao Hayashi*, «Development of remote pipe cutting tool for divertor cassettes in JT-60SA,» Fusion Engineering and Design, vol. 89, n. pagg. 2299–2303, 2014.
- [5] S. S. A. S. K. S. W. K. O. T. M. Takao Hayashi, «Development of remote pipe welding tool for divertor cassettes in JT-60SA,» Fusion Engineering and Design, vol. 101, n. Pagg. 180-185, 2015.
- [6] M. T. G. M. A. I. Takao Hayashi, «In-bore laser welding tool for actively cooled divertor cassettes in JT-60SA,» Fusion Engineering and Design, vol. 177, 2022.
- [7] T. M. Y. N. N. T. K. Hisashi Tanigawa, «Laser welding to expand the allowable gap in bore welding for ITER blanket hydraulic connection,» Fusion Engineering and Design, Vol. 1 di 298-99, n. Pagg. 1634–1637, 2015.